Electronic Supplementary Information – Timing performance of lead halide perovskite nanoscintillators embedded in polystyrene matrix

Kateřina Děcká,[a b] Fiammetta Pagano,*[c d] Isabel Frank,[c e] Nicolaus Kratochwil,[c] Eva Mihóková,[a b] Etiennette Auffray[c] and Václav Čuba[a]

S1 Details on sythesis

S1.1 Chemicals

Cs_2CO_3 (99.9 %, Sigma-Aldrich), $PbBr_2$ (99.999 %, Sigma-Aldrich), oleylamine (OAm, 70 %, Sigma-Aldrich), oleic acid (OA, 90 %, Sigma-Aldrich), 1-octadecene (ODE, 90 %, Sigma-Aldrich), toluene (99.8 %, Sigma-Aldrich), n-hexane (anhydrous, 98 %, Sigma-Aldrich), didodecyldimethylammonium bromide (DDAB, 98 %, Sigma-Aldrich), ethylacetate (p. a., PENTA), polystyrene (PS, no additives, Nuvia, $M_n = 62$ kg/mol; $M_w = 338$ kg/mol). All chemicals were used as received without further purification, unless stated otherwise.

S1.2 $CsPbBr_3$ synthesis

To synthesize $CsPbBr_3$ nanocrystals, the standard hot-injection (HI) procedure introduced in reference [1] was used. The preparation of cesium oleate was modified to increase Cs:OA ratio in the reaction to 1:5 to achieve its better solubility at room temperature [2]. In short, 0.2760 g of $PbBr_2$, 20 mL of 1-octadecene (ODE), 2 mL of oleylamine (OAm), and 1.78 mL of oleic acid (OA), were mixed in 100 mL 3-necked flask and degassed at 110 °C under vacuum for 1 h. After that, 0.5 mL of degassed pre-synthesized cesium oleate solution (0.4M) was injected at 170 °C under argon atmosphere. More details on the $CsPbBr_3$ synthesis can be found in our previous publication [3].

Synthesized $CsPbBr_3$ nanocrystals were precipitated by centrifugation, and radioluminescence (RL) spectra were measured on the sample precipitate. The precipitate was redispersed in either n-hexane for the photoluminescence (PL) characterization (for its preferable optical properties), or toluene for the embedding procedure. The toluene solution concentration was adjusted to ≈50–60 mg/mL. The concentration was determined spectrophotometrically at 400 nm [4].

S1.3 Ligand exchange

Ligand exchange reactions were performed at room temperature in air following the procedure presented in reference [5]. The crude reaction mixture in ODE from the HI synthesis was mixed with 55 mM DDAB toluene solution (volume ratio 3:2) and after vigorous stirring, the nanocrystals were precipitated by addition of ethyl acetate (volume ratio 5:1) and isolated by centrifugation (10 minutes at 4800 × g). For more details, see reference [6].

The precipitate was either re-dispersed in toluene for further experiments, or in n-hexane for PL characterization. The RL spectra were measured on the sample precipitate.

The toluene solution concentration was, as before, adjusted to ≈50–60 mg/mL for the embedding procedure.

[a] *Faculty of Nuclear Sciences and Physical Engineering, Czech Technical University in Prague, Břehová 7, 115 19 Prague, Czech Republic*
[b] *Institute of Physics of the Czech Academy of Sciences, Cukrovarnická 10, 162 53 Prague, Czech Republic*
[c] *CERN, Esplanade des Particules 1, 1211 Meyrin, Switzerland*
[d] *Università degli Study Milano Bicocca, Piazza dell'Ateneo Nuovo, 1-20126 Milano, Italy*
[e] *LMU Munich, Geschwister-Scholl-Platz 1, 80539 Munich, Germany*
* Corresponding author, E-mail: fiammetta.pagano@cern.ch

S2 Supplementary data

S2.1 Free nanocrystals characterization

The ligand exchange procedure on $CsPbBr_3$ nanocrystals (DDAB for OA+OAm) did not affect the crystalline structure in any substantial way, as confirmed by XRPD measurements, shown in Figure S1. The average crystallite size was determined to be (10 ± 1) nm, which in this case also represents the size of individual nanocrystals [3].

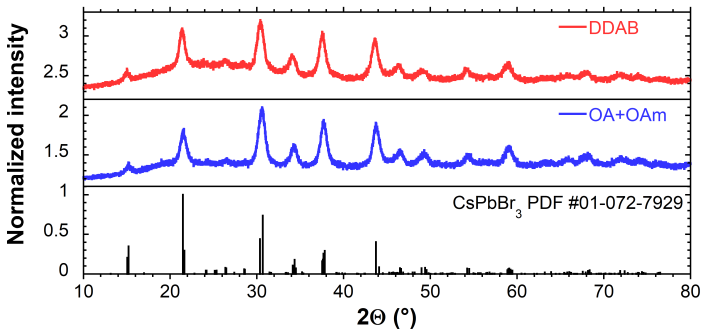

Fig. S1 XRPD pattern of $CsPbBr_3$ samples capped with DDAB (pink) and OA + OAm (blue) compared to the PDF card for orthorhombic $CsPbBr_3$.

As evidenced in Figure S2, both photoluminescence (PL) and radioluminescence (RL) intensities of free (not yet embedded in polysterene) $CsPbBr_3$ nanocrystals capped with DDAB were improved compared to the capping with OA+OAm. This is in agreement with our expectation, since DDAB is a quaternary ammonium salt which better passivates the nanocrystal surface [5].

For both sets of samples, we observed a red-shift between the PL and RL spectra; from 514 ± 0.5 nm in PL to 528 ± 0.5 nm in RL for the OA+OAm capped nanocrystals and from 514 ± 0.5 nm in PL to 529 ± 0.5 nm in RL for the DDAB capped nanocrystals. Similar (and even more pronounced) shift was observed also in PL spectra, see Figure S4.

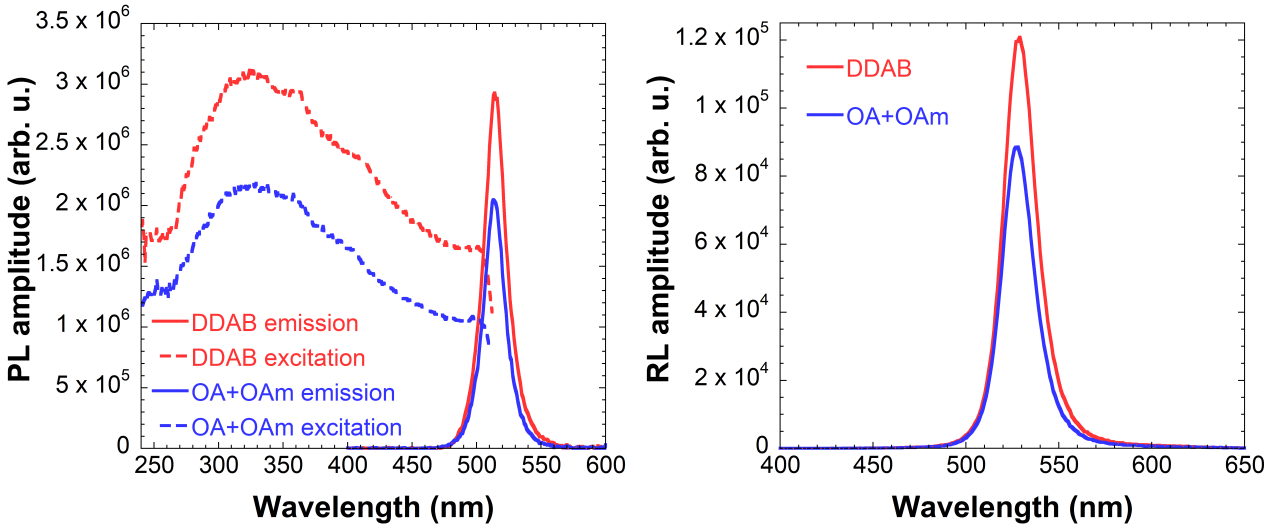

Fig. S2 Left: PL excitation (dashed line) and emission (solid line) spectra of $CsPbBr_3$ samples capped with DDAB (pink) and OA + OAm (blue). Right: RL spectra of $CsPbBr_3$ samples capped with DDAB (pink) and OA+OAm (blue).

S2.2 Fitting procedure of emission maxima

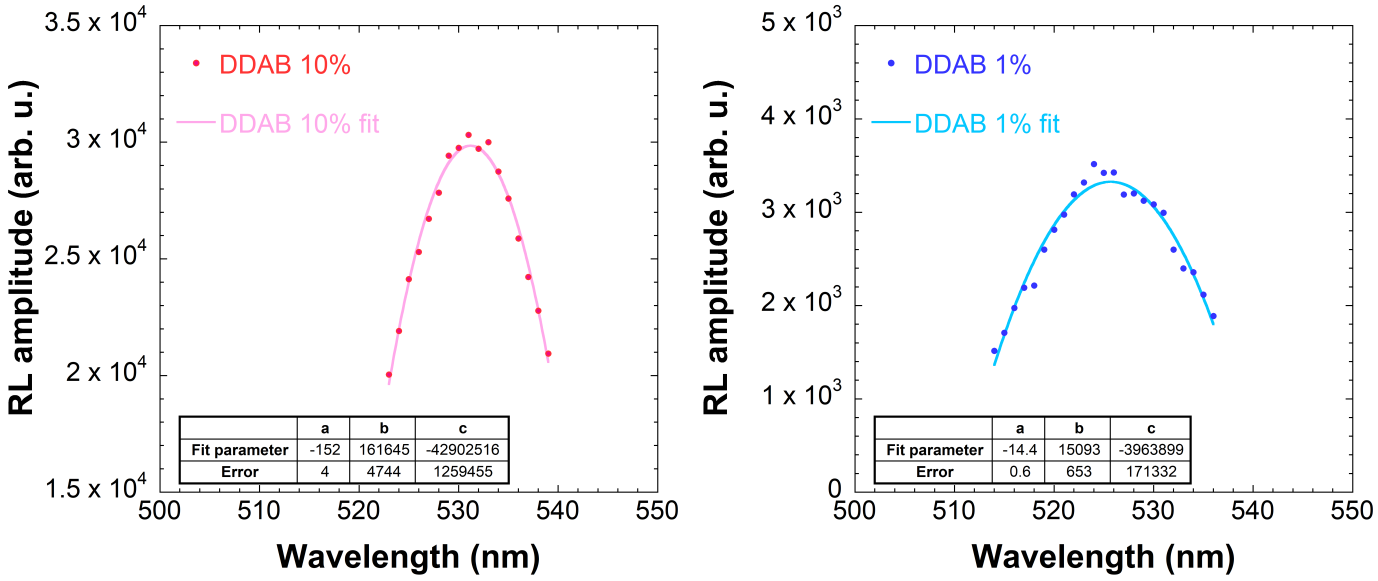

Fig. S3 Examples of the radioluminescence emission spectrum fit around its maximum, 10% (left) and 1% (right) filling factors of the DDAB set are shown. The experimental data around emission maximum were fitted using a quadratic function $y = ax^2 + bx + c$. Obtained fit parameters and their standard errors are displayed in the insets.

S2.3 RL and PL emission maxima positions

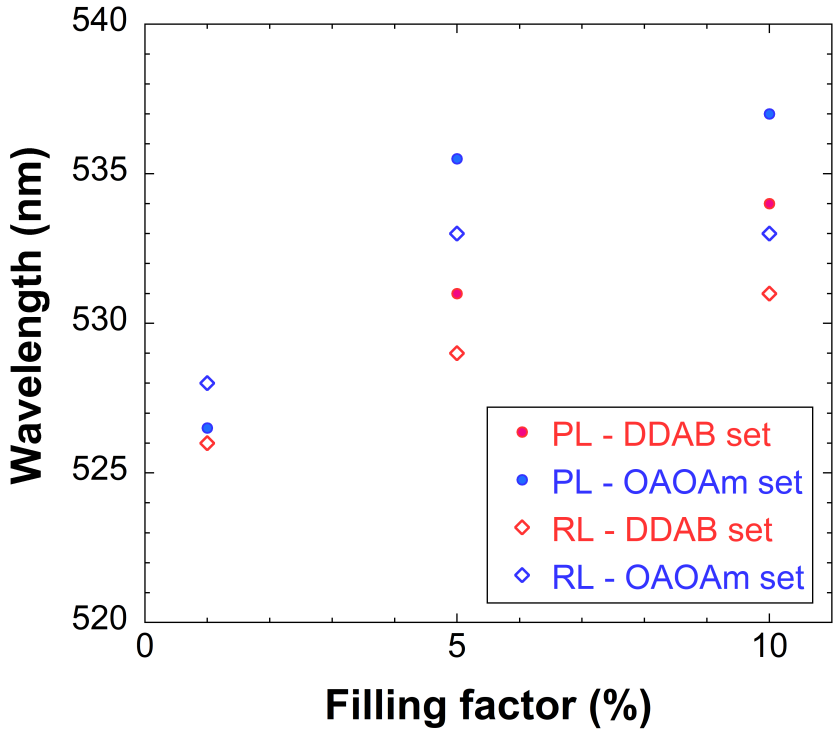

Fig. S4 Positions of emission band as a function of the filling factor. Circles and diamonds represent photoluminescence and radioluminescence data, respectively. Pink and blue color stand for DDAB and OA+OAm set, respectively.

S2.4 Stability

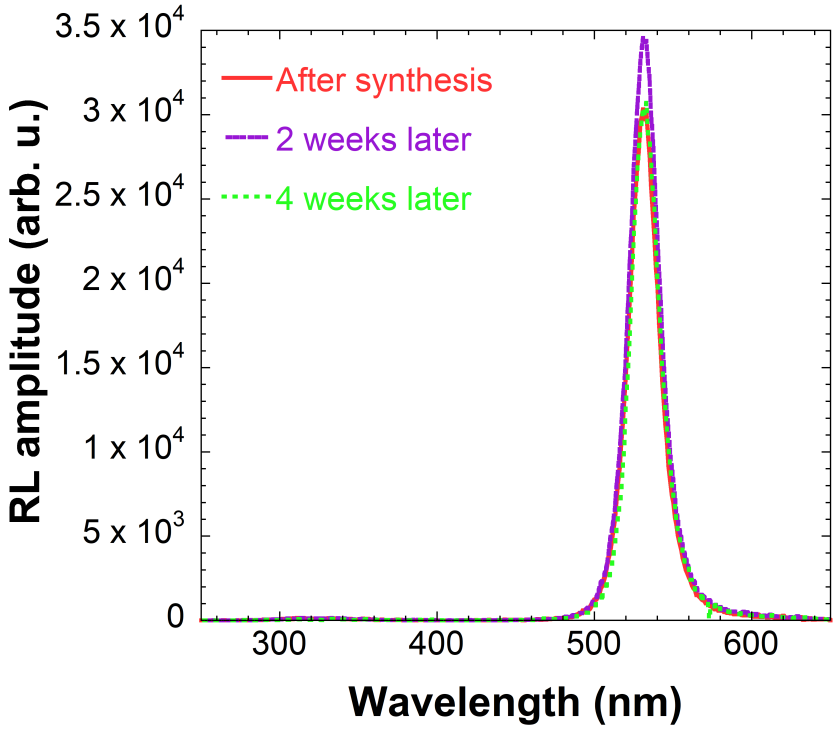

Fig. S5 Radioluminescence spectra of 10% sample of the DDAB set measured over the course of 1 month. The slightly larger intensity of the second measurement is not significant; it could have been caused by the slight change in geometry while measuring either the nanocomposite sample or the used standard sample.

S2.5 Scintillation decay kinetics

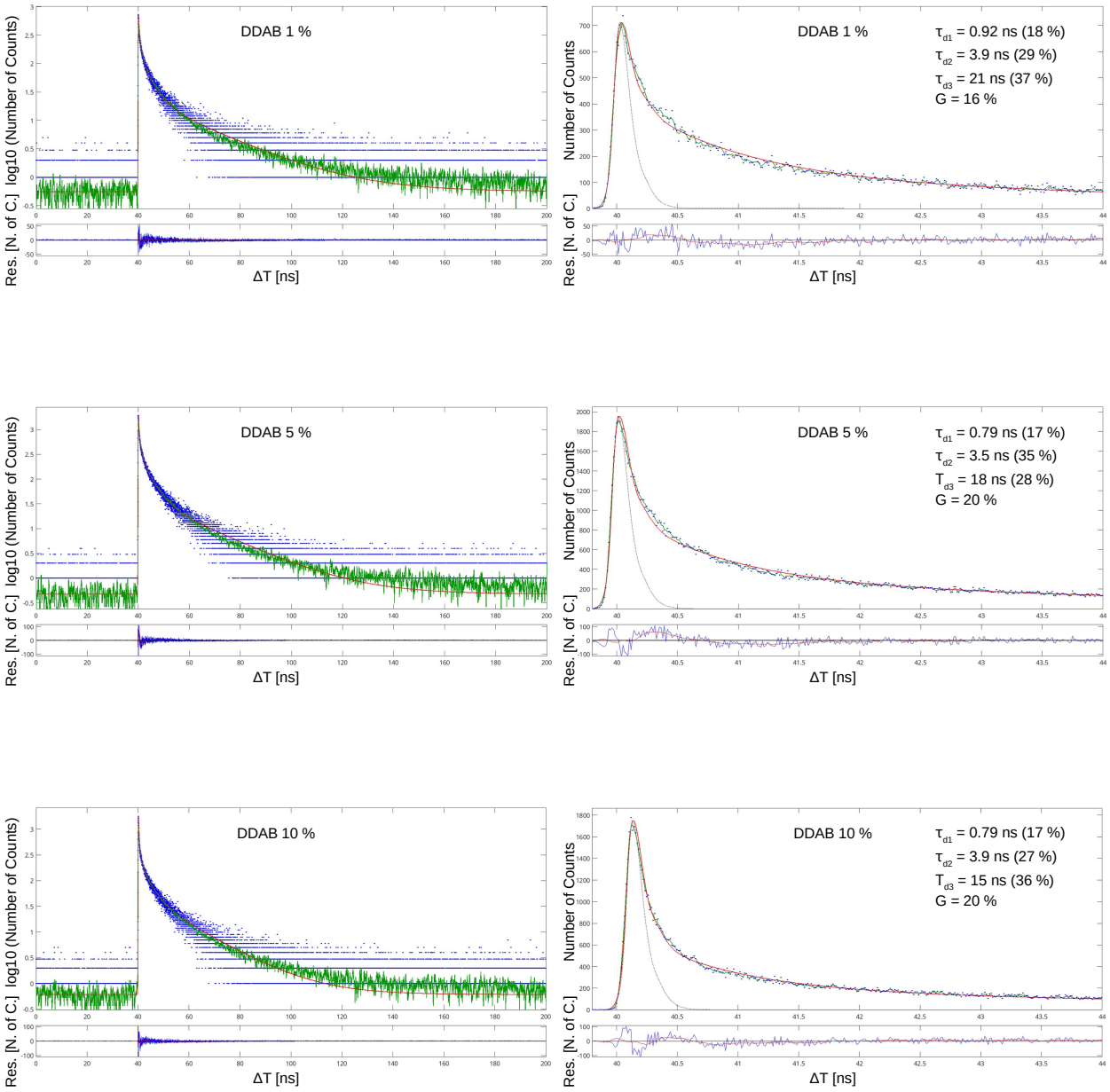

Fig. S6 Scintillation pulses of CsPbBr3 samples capped with DDAB. G is the weight of the delta function used to model the ultra-fast component, τ_{d1}, τ_{d2} and τ_{d3} are the exponential decay components of the fit with the respective weights (R_1, R_2 and R_3). Left: Scintillation decay shown in semi-logaritmic scale over the whole range ($\approx$ 150 ns). The blue dots are the measured data points, the green line the moving average, and the red curve is the fit function. Right: Detail of the ultra-fast component in linear scale. The dotted gray line represents the system IRF.

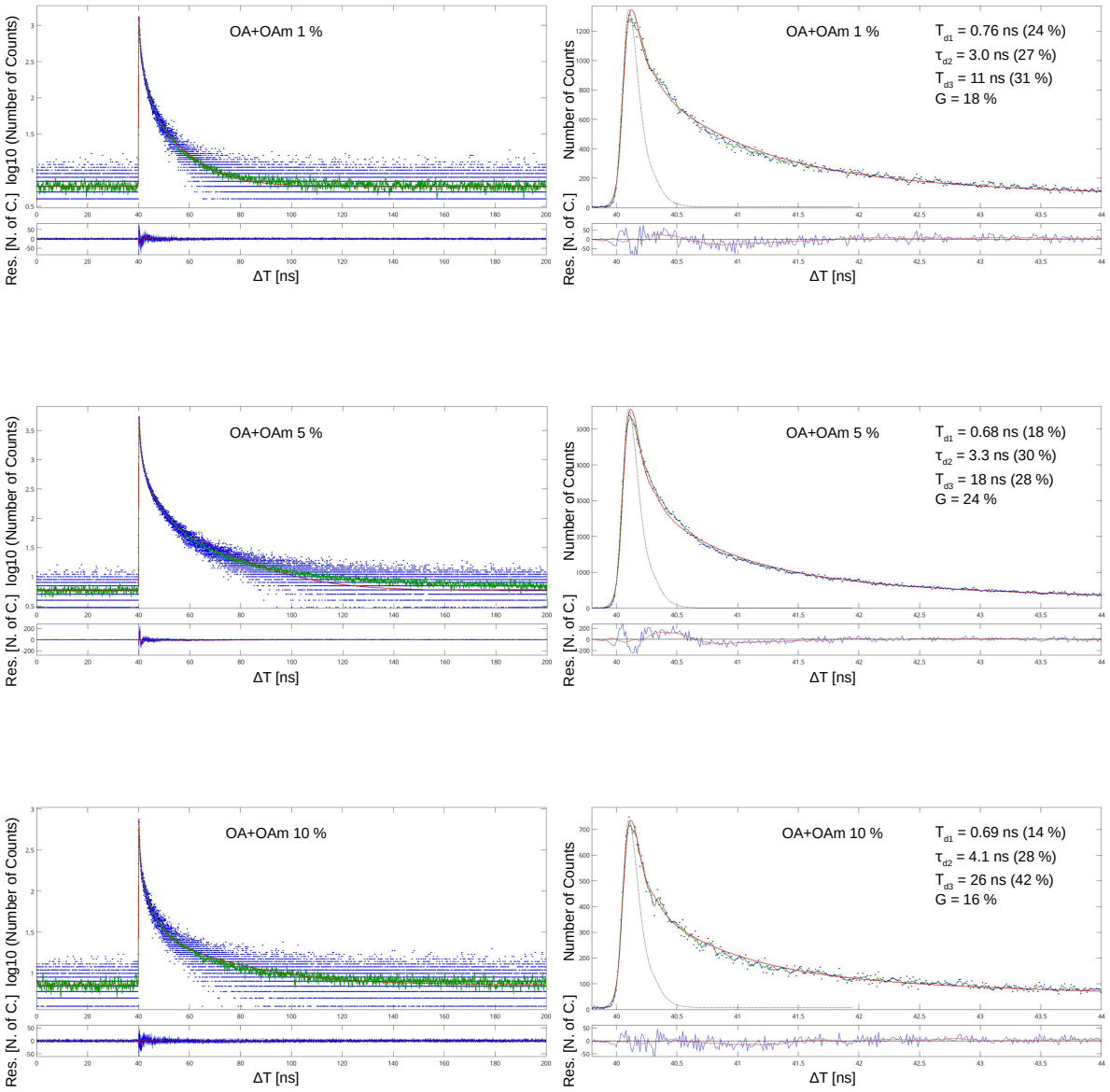

Fig. S7 Scintillation decays of CsPbBr3 samples capped with OA+OAm. G is the weight of the delta function used to model the ultra-fast component, τ_{d1}, τ_{d2} and τ_{d3} are the exponential decay components of the fit with the respective weights (R_1, R_2 and R_3). Left: Scintillation decay shown in semi-logaritmic scale over the whole range ($\approx$ 150 ns). The blue dots are the measured data points, the green line the moving average, and the red curve is the fit function. Right: Detail of the ultra-fast component in linear scale. The dotted gray line represents the system IRF.

S2.6 Detector time resolution upon X-ray excitation

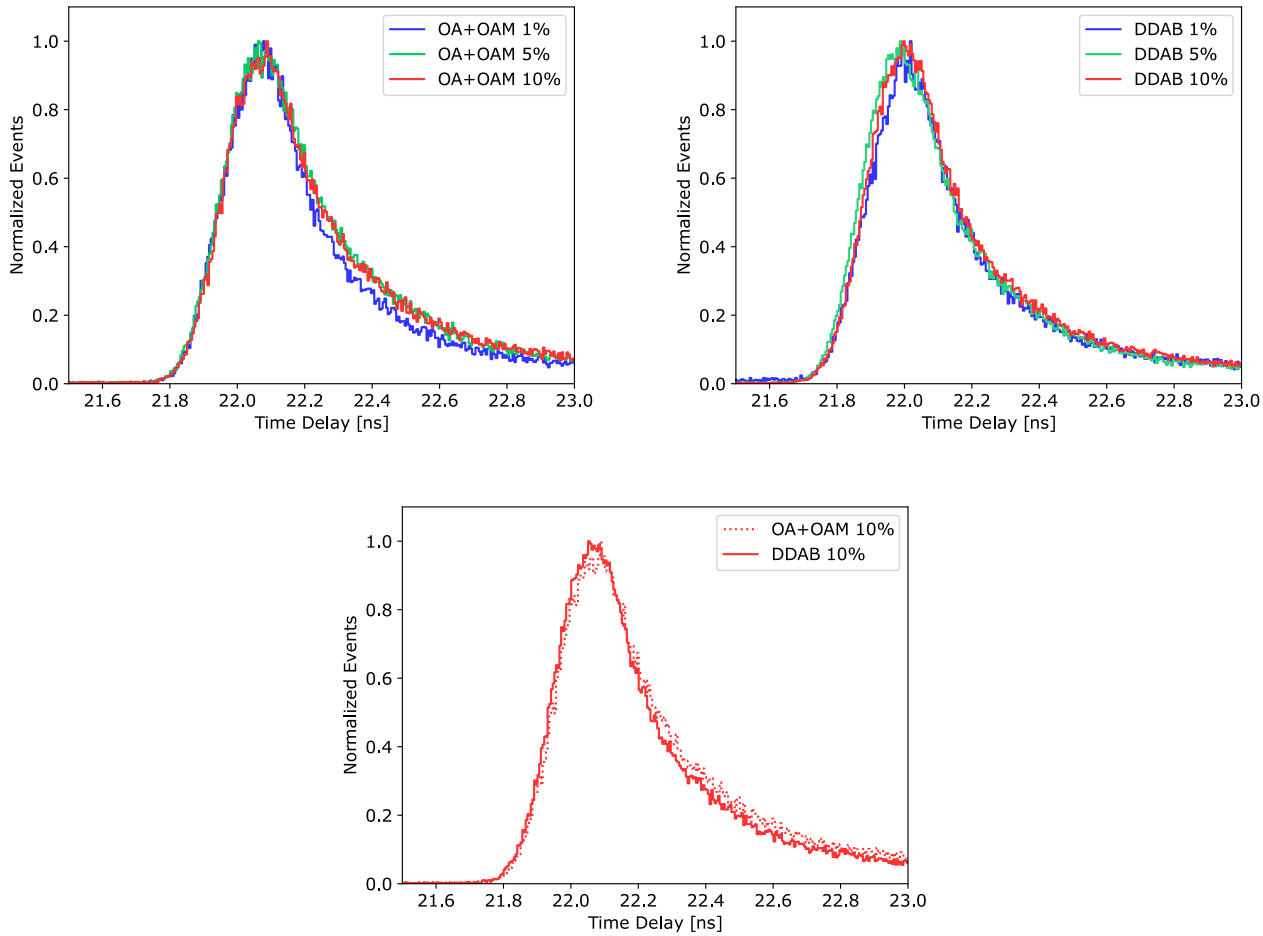

Fig. S8 Comparison of the time delay distributions: samples with three different filling factors of the OA+OAm set (upper left), DDAB set (upper right), and two samples with 10% filling factor of both sets (bottom).

S3 Supplementary discussion

S3.1 Production quality

A difference between the two sets of nanocomposite samples can be already observed from the characterization of free nanocrystals: RL and PL have higher intensities for $CsPbBr_3$ capped with DDAB (see Figure S2). When comparing PL and RL spectra of free nanocrystals in Figure S2, there is a clear red-shift of 15 nm in RL with respect to PL. This red-shift is caused by a different excitation mechanism. In RL, larger nanocrystals (emitting at longer wavelengths due to the quantum confinement effect) are excited with higher probability. Moreover, it is likely that larger nanocrystals in the sample re-absorb and re-emit the emission of the smaller nanocrystals, which also contributes to the observed red-shift.[7]

Compared to the OA+OAm set, better optical properties were observed for the DDAB set also after embedding in polystyrene: a better transparency of these samples, already visible by naked eye especially for high filling factors (cf. photographs in Table 1), was confirmed by transmission measurements (see Figure 1). When comparing samples with 5 and 10 % filling factor to the one with 1 % filling factor, it is significant that for the first two the drop to zero occurs at 525 nm (corresponding to absorption edge of larger nanocrystals), while for the latter a transmission of $\approx$10 % is observed up to 275 nm (the absorption edge of polystyrene). Clearly, the optical properties are dictated by polystyrene in case of 1 % samples in both sets, and by $CsPbBr_3$ nanocrystals themselves for higher filling factors. Moreover, looking at the general drop in the transmission of nanocomposites with higher filling factors, the nanocrystals seem to be aggregated there. Because of that, we expect that self-absorption issues may occur in these samples, which is usual for this type of nanocrystals (i. e. semiconductor quantum dots). This phenomenon should manifest as a red-shift in RL spectra and should also affect decay kinetics; see the respective parts in the "Clustering and aggregation" section of discussion below.

Moreover, the Petri dish from the experiment with 10% filling factor (picture at the bottom right of DDAB columns in Table 1) showed no $CsPbBr_3$ residue, in contrast with the presence of small $CsPbBr_3$ residue in the Petri dish from the experiment using OA+OAm (picture at the bottom right of OA+OAm columns in Table 1). These results are in agreement with our expectation, since DDAB is a quaternary ammonium salt which better passivates the nanocrystal surface.

We conclude that DDAB ligand, while increasing the luminescence intensities of free nanocrystals, also enables to achieve higher filling factors (up to 10 %) in the polystyrene matrix while maintaining better transparency of such nanocomposites. In contrast, 10 % filling factor was clearly not achieved for OA+OAm capped nanocrystals.

S3.2 Clustering and aggregation

Better surface passivation should also result in better prevention from nanocrystal aggregation. On the basis of the obtained results, we can make some consideration in this regard. First, we would like to distinguish the simple *clustering* - i.e. nanocrystals forming larger clusters but preserving their shape and size - from real *aggregation* - i.e. nanocrystals forming bigger particles with their neighbours. Naturally, the aggregation can be understood as an extreme case of simple clustering (first, nanocrystals undergo clustering process and then aggregation may occur).

The low transmittance above 525 nm for samples with 5 % and 10 % filling factors suggests that at least some level of clustering is occurring in both sets. However, as already mentioned, the effect seems to be lower for nanocrystals capped with DDAB.

The observed slight red-shift in RL spectra with increasing filling factor (even more pronounced in PL spectra, see FigureS4) is traceable to both phenomena as well, but also the simple fact of more nanocrystals present in the matrix contributes to it. Also, with rising filling factor, the probability of having clustering (and possible aggregation) is getting higher. Consequently, larger nanoparticles (either already present or created by aggregation) can absorb the light emitted by smaller and non-aggregated nanocrystals, and re-emit at longer wavelengths. This is the first confirmation of our expectation based on optical properties observed in transmission spectra.

The self-absorption suggests that also some level of aggregation, not only clustering, is present in our samples. However, to understand how significant it is, we need to look at scintillation decay kinetics. Because of the quantum confinement effect, it is indeed expected that, if a significant number of larger nanocrystals is formed by aggregation, slower decay time - or at least higher weights of longer decay components - at the expense of the faster ones should be observed. This tendency was clearly observed only for samples belonging to the OA+OAm set: the slowest decay component increases from 11 ± 1 ns (contributing for 31 ± 7 %) to 26 ± 3 ns (contributing for 42 ± 7 %) as the filling factor increases from 1 % to 10 %, at the expense of the fastest exponential decay components, whose contribution drops from 24 ± 4 % to 14 ± 2 %. This trend in the OA+OAm set is also confirmed by the effective decay time, which provides an understanding of the overall decay time instead of the individual components. On the contrary, the DDAB set did not result significantly affected by the increasing filling factor.

The presented results confirm our expectation based on tramsmission spectra about possible self-absorption (in both sets) and aggregation (only for OA+OAm set). Morover, they support our previous conclusion about the better capability of DDAB ligand of lowering the level of nanoparticles clustering and almost suppressing the aggregation.

S3.3 Luminescence quenching

Another observed effect related to the presence of larger nanoparticles is the luminescence quenching. Despite no reduction of luminescence intensity was observed with rising filling factor, luminescence quenching usually manifests also as a speed-up of the scintillation decay kinetics, most probably by faster decay times. This was indeed observed for both sets of nanocomposites. For the OA+OAm set, the fastest exponential decay component dropped from 0.76 ± 0.02 ns for 1% filling factor to $0.68(9) \pm 0.02$ ns for higher filling factors and for the DDAB set, from 0.92 ± 0.03 ns for 1% filling factor to 0.79 ± 0.02 ns for higher filling factors.

This speed-up of scintillation response might be also resulting from non-radiative energy transfer (FRET) between neighbouring nanocrystals in their clusters. However, it would require much more detailed analysis, which was beyond the scope of this article.

Overall, our results suggest that every phenomenon discussed above is most probably present in all of our samples, competing with each other (e. g. slower decays due to aggregation vs. faster decays due to quenching, lower luminescence intensities due to quenching and light scattering vs. higher luminescence intensities because more emittors are present in the sample). However, emission spectra of both free and embedded nanocrystals, and transmission spectra suggest that the DDAB surface ligand, compared to OA+OAm, better prevents $CsPbBr_3$ nanocrystals from aggregating within the polystyrene matrix. Only thorough analysis of the decays could reveal that overall, despite the quenching, the DDAB set performed slightly better (i. e. gave more stable results for higher filling factors). Most importantly, it seems that the DDAB ligand supports higher filling factor, which means higher stopping power and on average more energy deposition (thus more light) in the nanocrystals, which is a key factor for the application.

Notes and references

1 L. Protesescu, S. Yakunin, M. I. Bodnarchuk, F. Krieg, R. Caputo, C. H. Hendon, R. X. Yang, A. Walsh and M. V. Kovalenko, *Nano letters*, 2015, 15, 3692–3696.

2 C. Lu, M. W. Wright, X. Ma, H. Li, D. S. Itanze, J. A. Carter, C. A. Hewitt, G. L. Donati, D. L. Carroll, P. M. Lundin *et al.*, *Chemistry of Materials*, 2018, 31, 62–67.

3 K. Děcká, A. Suchá, J. Král, I. Jakubec, M. Nikl, V. Jarỳ, V. Babin, E. Mihóková and V. Čuba, *Nanomaterials*, 2021, 11, 1935.

4 J. Maes, L. Balcaen, E. Drijvers, Q. Zhao, J. De Roo, A. Vantomme, F. Vanhaecke, P. Geiregat and Z. Hens, *The journal of physical chemistry letters*, 2018, 9, 3093–3097.

5 M. Imran, P. Ijaz, L. Goldoni, D. Maggioni, U. Petralanda, M. Prato, G. Almeida, I. Infante and L. Manna, *ACS Energy Letters*, 2019, 4, 819–824.

6 K. Děcká, J. Král, F. Hájek, P. Průša, V. Babin, E. Mihóková and V. Čuba, *Nanomaterials*, 2021, 12, 14.

7 K. Tomanová, A. Suchá, E. Mihóková, L. Procházková, I. Jakubec, R. M. Turtos, S. Gundacker, E. Auffray and V. Čuba, *IEEE Transactions on Nuclear Science*, 2020, 67, 933–938.